



From waste of marine culture to natural patch in cardiac tissue engineering

Yutong He^{a,1}, Honghao Hou^{a,1}, Shuqi Wang^{b,1}, Rurong Lin^a, Leyu Wang^c, Lei Yu^a, Xiaozhong Qiu^{a,*}

^a Guangdong Provincial Key Laboratory of Construction and Detection in Tissue Engineering Department of Anatomy, School of Basic Medical Sciences, Southern Medical University, Guangdong, Guangzhou, 510515, China

^b Guangdong Province Key Laboratory of Marine Biotechnology, Shantou University, Shantou, 515063, China

^c School of Biomedical Engineering, Southern Medical University, Guangzhou, 510005, China

ARTICLE INFO

Keywords:

Sea squirts
Biofouling
Cellulose
Cardiac tissue engineering
Myocardial infarction

ABSTRACT

Sea squirt, as a highly invasive species and main biofouling source in marine aquaculture, has seriously threatened the biodiversity and aquaculture economy. On the other hand, a conductive biomaterial with excellent biocompatibility, and appropriate mechanical property from renewable resources is urgently required for tissue engineering patches. To meet these targets, we presented a novel and robust strategy for sustainable development aiming at the marine pollution via recycling and upgrading the waste biomass-sea squirts and serving as a renewable resource for functional bio-scaffold patch in tissue engineering. We firstly demonstrated that the tunic cellulose derived natural self-conductive scaffolds successfully served as functional cardiac patches, which significantly promote the maturation and spontaneous contraction of cardiomyocytes both in vitro and enhance cardiac function of MI rats in vivo. We believe this novel, feasible and “Trash to Treasure” strategy to gain cardiac patches via recycling the waste biomass must be promising and beneficial for marine environmental bio-pollution issue and sustainable development considering the large-scale consumption potential for tissue engineering and other applications.

1. Introduction

Aquaculture is one of most important leading industries in offshore countries and areas. With the boom of marine aquaculture in recent years, biofouling induced by overpopulation of some marine culturing concomitants is becoming a bigger and bigger concern for ecological environment, biodiversity, and economic efficiency of aquaculture as well [1]. For example, during massive cultivation of scallops, it is being threatened by the invasive tunicate of sea squirts, which have become invasive and overpopulated, can quickly overgrow an area, replacing native species and becoming one of major trouble restricting the sustainable development of aquaculture industry and marine ecological environment [2]. However, this biofouling issue caused by excessive marine growth in marine culturing systems is a heavy work and extremely difficult to be disposed with [3]. Most of sea squirts without any value and often are abandoned as wastes. For preventing the sea squirts attaching the cages, a lot of scallop and mussel growers are trying

to keep their culturing cages or mussels socks clean by either injecting high-pressure water or lime solution, which cost farmers more than 30% of their farm total operational costs annually including the capital cost of the equipment [2]. Nearly 50–60 wt % of the biomass generated during the processing of shellfish is waste, and the uncontrolled dumping of this biomass, is a serious environmental problem [4,5]. So how to take advantage of the “potentials” of these excessive biological contaminations and develop a facile, economical, “Trash to Treasure” approach which can effectively upgrade from these renewable and even waste resources is fantastic and interesting.

At the other hand, the invasive tunicates, sea squirts, can be regarded as a natural, prolific and economical sources of cellulose and new chemical entities with unique structures and potent biological activities [6]. The outer tissues of tunicate (termed tunic) is comprised of cellulose microfibrils, which acts as a skeletal structure, and can be isolated to produce cellulose. As we know, cellulose is the most abundant natural polymer on earth, and gains an increasing interest recently, as the demand for an alternative to non-renewable fossil fuel-based resources has

Peer review under responsibility of KeAi Communications Co., Ltd.

* Corresponding author.

E-mail address: qiuxzh@smu.edu.cn (X. Qiu).

¹ These authors contributed equally to this work.

<https://doi.org/10.1016/j.bioactmat.2020.12.011>

Received 10 October 2020; Received in revised form 12 December 2020; Accepted 12 December 2020

2452-199X/© 2020 The Authors. Production and hosting by Elsevier B.V. on behalf of KeAi Communications Co., Ltd. This is an open access article under the CC

BY-NC-ND license (<http://creativecommons.org/licenses/by-nc-nd/4.0/>).

Abbreviations

MI	Myocardial infarction
ECM	Extracellular matrix
PBS	Phosphate buffered saline
Ppy	Polypyrrole
EDS	Energy dispersive spectroscopy
XRD	X-ray diffraction
AFM	Atomic force microscope
RMS	Root-mean-square
ANOVA	One-way analysis of variance
CMs	Cardiomyocytes
CX-43	Connexin 43
CCK-8	Cell Counting Kit-8

LAD	Left anterior descending
SD	rats Sprague-Dawley rats
FS	Short axial shortening
EF	Ejection fraction
ECP	Engineered cardiac patch
ESV	End systolic volume
EDV	End diastolic velocity
α -SMA	Alpha smooth muscle Actin
vWF	von willebrand factor
DTG	Thermogravimetric analysis
SEM	Scanning electron microscope
FTIR	Fourier transform infrared spectra
PTC hydrogel	Pyrrole modified cellulose hydrogel

increased [7]. The over-reproducing ocean farming waste provides an abundant and accessible source of tunicate feedstock. It is promising that via the bio-engineering refinement of tunicates for cellulose production and effective utilization of biomass, we could potentially reduce the tunicate associated problems in farming scallops and mussels, while creating new economic opportunities moving towards bio-economy and addressing the threaten for biodiversity and sustainable development. To date, sea squirt has been utilized to extract bioactive substances, such as alkaloids, purines, cyclic peptide, and indoles [8]. Particularly, the animal-derived celluloses exhibit some similarities of homologous microstructure with the myocardial fibers of human cardiac tissue, while the tunic tissue is the only known animal source of cellulose among all natural cellulose sources. Compared with the plant cellulose, the animal-resource cellulose exhibits higher molecular weight, stronger mechanical properties, water holding capacity, water and air permeability and better thermal stability [9], enabling some unique advantages and potentials in tissue engineering. Although there have been some studies using cellulose-based materials for myocardial reparation, which were not involved in any *in vivo* experimental studies in almost all of publications [10–12]. Until now, the application of sea squirt in cardiac tissue engineering has not been exploited.

Cardiovascular diseases are the chief causes of death worldwide, with a significant proportion of deaths due to the myocardial infarction (MI) [13,14]. The cardiac tissue engineering is emerging as a potential approach to the myocardial repairing and regeneration via producing functional patches, which can bridge the healthy and MI region, and thus support the structural integrity and regeneration of tissues in MI mainly via a mechanism of electrical integration [15,16]. Despite much achievement of these tissue engineering patches for MI repair, the long-term safety and biocompatibility of non-biodegradable and non-homologous materials still remain a big concern due to the bio-toxicity and body rejection. Usually, most of these patch scaffolds are required to undergo a certain synthetic procedure to form and maintain a stable structure by either chemical or physical interactions [17], which inevitably introduced non-biodegradable and non-homologous materials. In addition, considering that the heart tissue is constituted with extracellular matrix (ECM) and highly oriented cells, bio-mimicking the anisotropic structure of cardiac tissue and guiding cellular orientation play a key role in designing cardiac patch for MI repairing. Although some attempts have been made in the design of anisotropic scaffold materials, most operations are complicated and difficult to truly simulate the natural structure of the myocardium [18, 19]. In a word, for the myocardial tissue engineering, a natural, self-conductive, compatible, accessible scaffold materials with well-aligned nanofibers and abundant source is urgently needed and to be developed.

To meet these targets, originating from marine aquaculture waste, we upgraded the tunic of biological polluter-sea squirts, and obtained

natural cellulose hydrogel as the cardiac patch scaffold for myocardial repair and regeneration (Fig. 1). The tunic hydrogel with good biocompatibility, alignment and conductivity obtained through simple treatment from sea squirts without chemical or physical crosslinking, which exhibited significant performance gain in myocardial infarction regions. This is the first examine the effect of cellulose alone on the repair of myocardial infarction. It is also the first example of successful application of natural patch in cardiac tissue engineering using marine culturing waste derived biomaterial from a very sustainable source. This facile, efficient, and “Trash to Treasure” approach opens a new horizon for the construction of tissue engineering patches taking advantage of natural sources.

2. Materials and methods

2.1. The tunic scaffold crude-extracted from sea squirts

The sea squirts samples were taken from several scallop cages, where the scallops were cultivated for approximately 1 year, immediately placed into freezer bags and frozen. After thawed in a fume hood, the sea squirts samples were washed for more than 10 times with deionized water, gently removing the epidermis in direct contact with the outside world. Then the body of sea squirt was opened using a scalpel, separating the internal organs from the outer capsule. The obtained tunic was washed with substantial deionized water, and cut into pieces of $1 \times 1 \times 0.2 \text{ cm}^3$ for further bio-refinement. The crude extraction sample of sea squirt tunic was obtained as a yellow hydrogel.

2.1.1. The tunic hydrogel scaffold bio-refining from the tunic of sea squirts

To acquire tunic cellulose hydrogel from the crude extraction of sea squirts tunic, a modified acid-hydrolysis and Kraft-cooking combinational method is used to obtain the cellulose hydrogel and remove lipids, non-glucose sugar, ash and protein from tunic tissue. First of all, the sea squirt tunic was cut into slices and immersed in 5 wt% sulfuric acid solution for 72 h. Then the samples were washed with deionized water until pH = 7. Finally, the samples were treated with 8 wt% sodium hydroxide aqueous solution for 6 h, following being immersed in phosphate buffered saline (PBS) solution and washed with deionized water for several times to remove the remaining base. At the end of this process all that was left of the sea squirt tunic was a transparent cellulose hydrogel (named tunic hydrogel). The overall yield of tunic and tunic hydrogel are $60 \pm 7\%$ and $75 \pm 5\%$, respectively, by calculating the ratio of mass of obtained solid, to initial mass of every step. The obtained tunic hydrogel could be directly used without any additional processes.

2.2. Preparation of pyrrole modified cellulose hydrogel (PTC hydrogel)

Considering the requirement of electrical conductivity, we prepared

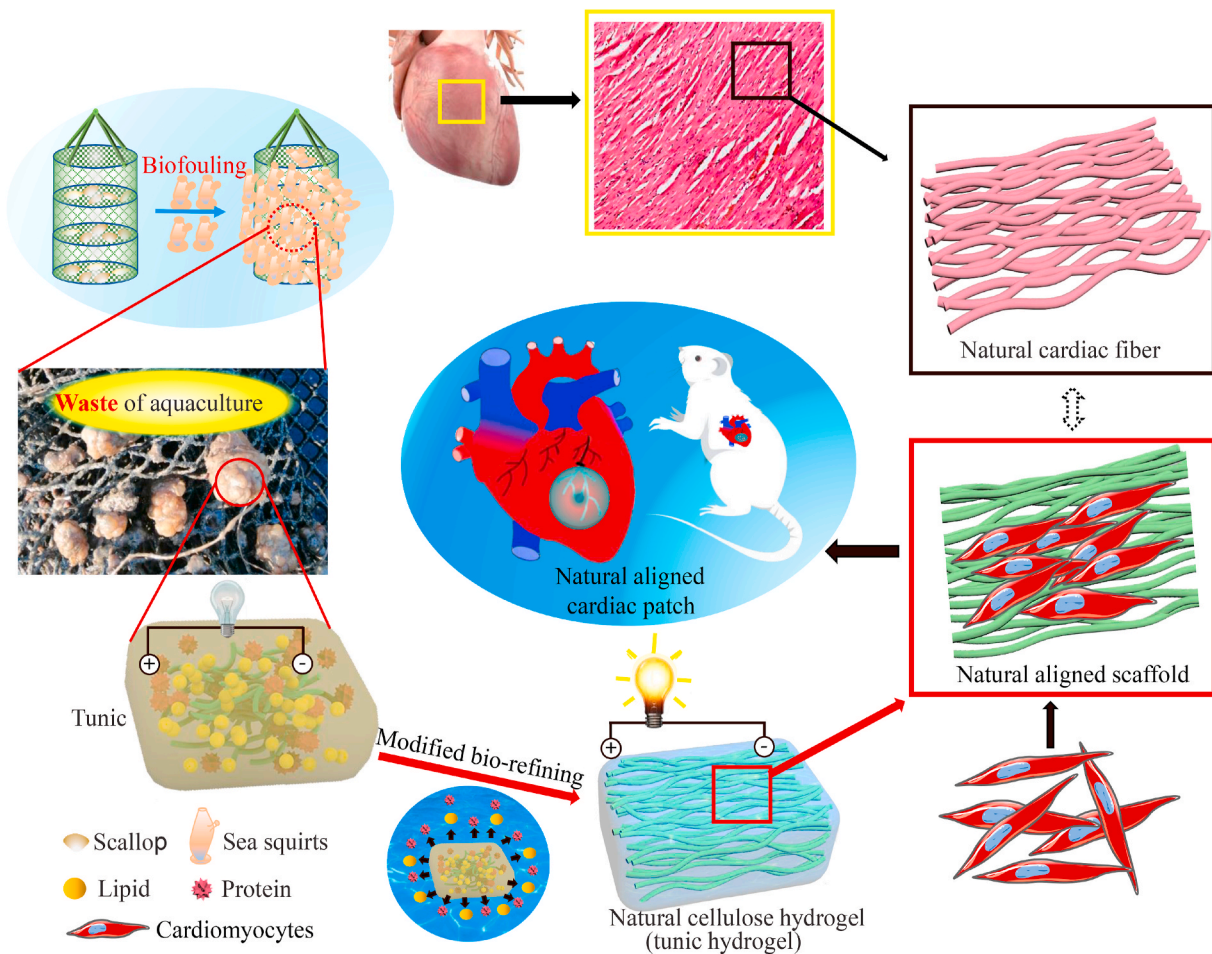


Fig. 1. The sea squirts-derived cardiac patch for myocardial infarction from waste of marine culture. The sea squirts, the waste of marine culture, could form the conductivity and well-aligned hydrogel after treating with acid and alike and significantly enhance the cardiac function of myocardial infarction rats.

a high-conductive hydrogel by in-situ polymerizing pyrrole on the surface of tunic hydrogel. The as-prepared tunic hydrogels were immersed in a freshly prepared pyrrole aqueous solution (0.5 mg/mL, 1 mg/mL, 2 mg/mL) in 4 °C for 12 h to ensure penetration equilibrium of pyrrole into the hydrogel networks. The pyrrole monomer loaded hydrogels were subsequently transferred into a FeCl_3 aqueous solution (0.3 mol/L) in 4 °C for 12 h to complete the polymerization *in situ*. After that, the hydrogels were rinsed thoroughly with deionized water to remove the residual chemical reagents, and the black and conductive Ppy *in-situ* modified tunic cellulose hydrogels (named PTC hydrogel) were obtained.

2.3. Characterization of tunicate cellulose-derived conductive hydrogel

The morphologies and sizes of cellulose hydrogel were observed by scanning electron microscope (SEM, H-7650, Hitachi, Japan). Fourier transform infrared spectra (FTIR) of the samples were collected with a FTIR spectrometer (Thermo Electron Instruments Co., Ltd., USA) in the frequency range of 4000–400 cm^{-1} with a total of 32 scans and resolution of 4 cm^{-1} . The thermal stability of the cellulose hydrogels was determined with a thermal gravimetric analyzer (NETZSCH TG 209F1 Iris). The element content of hydrogel was obtained by Energy Dispersive Spectroscopy (EDS, S-3000 N, Hitachi, Japan). The crystalline structures of tunic, tunic hydrogel and PTC hydrogel were analyzed by X-ray diffraction (XRD). Atomic force microscope (AFM, Bruker Dimension ico) was used to measure the root-mean-square (RMS) surface roughness (Rq) of tunic, tunic hydrogel and PTC hydrogel. The mechanical properties of different scaffolds were studied by

compression test with LS1 materials testing system (AMETEK, America), compressive ramp up to 80% strain and strain rate of 10% per minute, preload of 0.05 N was used.

2.4. The detection of biocompatibility and function of cardiomyocytes on different scaffolds

Primary cultured cardiomyocytes (CMs) were isolated from the hearts of 2-day old Sprague-Dawley rats according to a typical method reported by our group [20]. In brief, the hearts were carefully dissected and dissociated into single-cell suspensions with 0.1% collagenase type II (Sigma). Then the suspended cells were centrifuged at 1000 rpm for 5 min, and the harvested cells were pre-plated to separate CMs from cardiac fibroblasts for 2 h. Finally, the unattached CMs were collected and centrifuged at 1000 rpm for 5 min. The CMs were seeded on different scaffolds for 7 days. In order to evaluate whether the three scaffolds were toxic to CMs, live/dead staining and CCK-8 assays of CMs seeded on pristine tunic, tunic hydrogel and PTC hydrogel were analyzed respectively. For function of CMs analysis, the expression of α -sarcomeric actinin (α -actinin) and connexin 43 (CX-43) were analyzed using immunofluorescent staining and Western-Blot test.

2.5. Establishment of myocardial infarction model

All animal experiments were performed under the ethics committee guidelines, and laboratory animals approved by Southern Medical University Animal Ethics Committee. First, the SD rats (age 7–8 weeks, 220 ± 20 g) were anesthetized with isoflurane and the ligation left

anterior descending (LAD) was finished according to the previous report [20]. In the sham group, only thoracotomy was performed without ligation of the left anterior descending. Then the SD rats with FS (short axial shortening) less than 30 were randomly divided into MI group, tunic hydrogel ECP and PTC hydrogel ECP groups (size:1 cm × 1 cm × 0.2 cm). Then, the as-prepared primary CMs from newborn SD rats were seed on scaffolds and cultured for 3 days to get the ECP. Finally, the ECP scaffolds with cultured CMs were implanted into the infarction area of the rats in the tunic hydrogel ECP and PTC hydrogel ECP group. All patches were carefully fixed to the infarct area by suture. Meanwhile in the sham group, secondary thoracotomy was accomplished according to the transplant group.

2.6. Statistical analysis

All results were analyzed with the SPSS22.0 and GraphPad prism 5 software. The data were expressed as means ± standard deviations (SD). Statistical analyses were performed using one-way analysis of variance (ANOVA). Tukey HSD post hoc testing was used as the post hoc correction to compare multiple groups.

3. Results and discussion

3.1. Preparation and characterization of the tunic cellulose hydrogel

To obtain the natural cellulose hydrogel from pristine tunic of sea squirts, the protein and lipid of tunic were dislodged using simple treatment (Fig. 2a). The crude-extracted pristine tunic of sea squirts is a hydrogel with opaque status and yellow color due to the existence of considerable lipids and proteins. After a simple treatment through a modified bio-refining method to remove proteins and lipids using 5 wt% sulfuric acid solution, 8 wt% sodium hydroxide aqueous solution and PBS solution for three times, respectively, a tunic hydrogel was directly obtained, which was transparent and soft (Fig. 2a). It is noted that we could get a tunic hydrogel directly through this modified bio-refining method, distinctly differing from typical methods for pure cellulose nanocrystalline or pure cellulose from sea squirt tunic [21]. This approach to direct upgrade the tunic hydrogel and is prevailing over other reported methods because it can remain the intrinsic physico-chemical and biologic properties of tunic cellulose. For comparison, considering the conductivity requirement, polypyrrole (Ppy) was further used to obtain a high conductive Ppy tunic hydrogel (noted by PTC hydrogel) prepared by in-situ polymerization of pyrrole on tunic

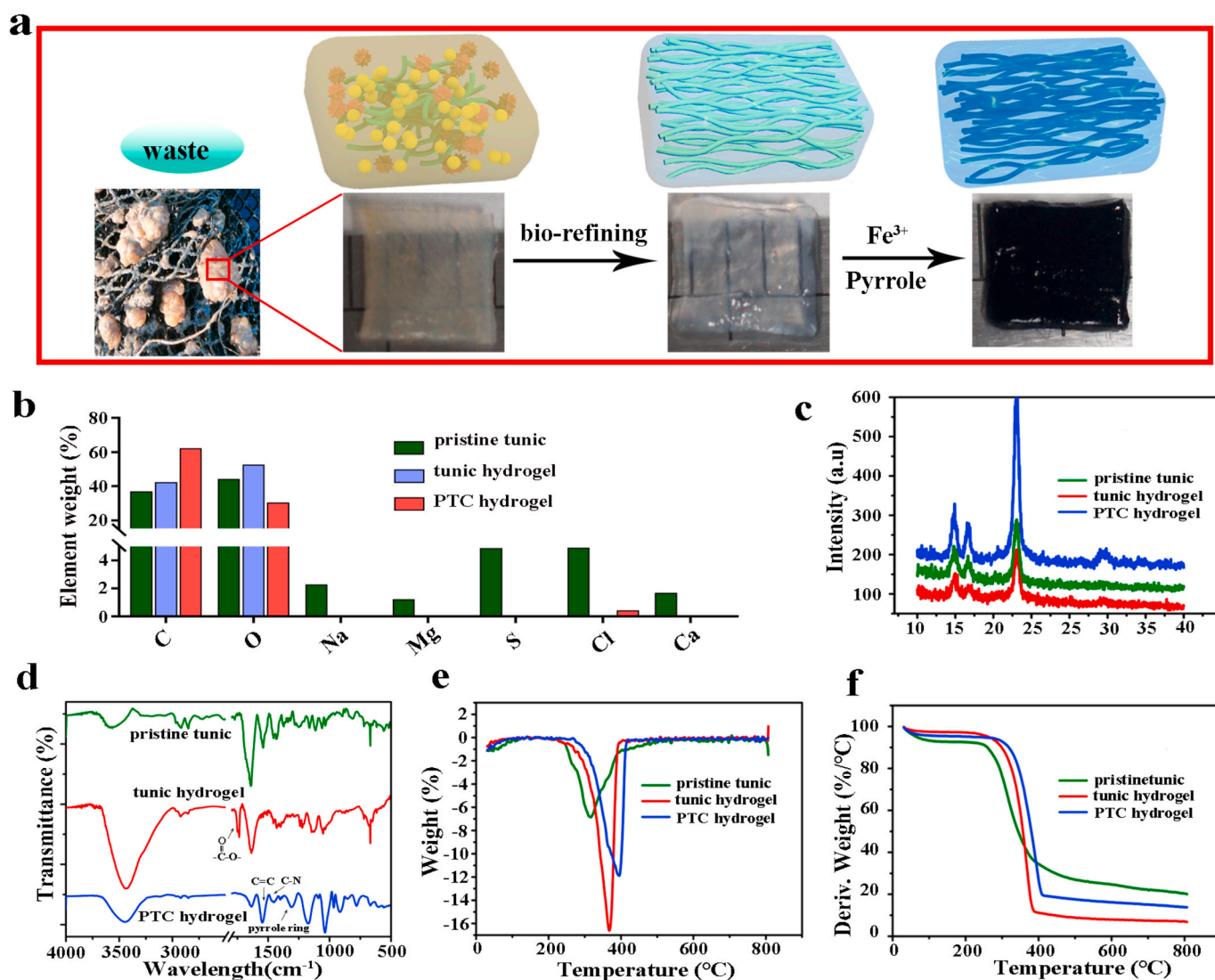


Fig. 2. The preparation of tunic cellulose hydrogel. (a) The preparation procedure of pristine tunic, tunic hydrogel and PTC hydrogel. (b) The elemental analysis of pristine tunic, tunic hydrogel and PTC hydrogel. (c) XRD analysis for pristine tunic, tunic hydrogel and PTC hydrogel. (d) FTIR spectra of pristine tunic, tunic hydrogel and PTC hydrogel. TGA (e) and DTG (f) curves of pristine tunic, tunic hydrogel and PTC hydrogel.

cellulose nanofibers (Fig. 2a). These naturally elastic and soft samples of pristine of sea squirt tunic and tunic hydrogel provides a premise and possibility for further direct application as patches in cardiovascular tissue engineering. Then we firstly used EDS element mapping to detect and analysis the chemical constituent and structure of these hydrogel samples (Fig. 2b). Without our treatment, the pristine tunic showed a complicated composition with over 81.28% of carbon and oxygen elements, and no more than 5% of microelement such as Si, S and Ca, which were key components of organism [22,23]. After treatment, the tunic hydrogel only contained carbon and oxygen (Fig. 2b), which is over 95%. However, the PTC hydrogel possessed vast carbon and oxygen as well as a little chlorine, the chlorine-doped endowed PTC hydrogels good electrical conductivity. After treatment with modified bio-refining method, the tunic hydrogel completely removes the protein, the lipid, leaving only the cellulose skeleton.

The successful fabrication of tunic cellulose-derived hydrogels was also confirmed by XRD analysis. The XRD curves of the pristine tunic, the tunic hydrogel and the PTC hydrogel showed strong crystalline peaks at 14.7° , 16.8° and 22.8° , corresponding to the (110), (110), and (200) crystal planes, respectively, which indicates a typical cellulose I structure [9] (Fig. 2c). Compared to the tunic hydrogel, the peak intensity of the pristine tunic and the PTC hydrogel decreased dramatically due to the effect of protein, lipid and Ppy. The high crystalline structure of tunic hydrogel may endow better electron conductivity over the pristine tunic [24]. FTIR analysis was applied to further verify the chemical structures of three different hydrogels (Fig. 2d). A strong absorption peak around 3408 cm^{-1} was corresponds to $-\text{OH}$ stretching vibration, and the peak distribution of tunic hydrogel was wider than that of pristine tunic, because of the association of $-\text{OH}$ with water. The absorption peak corresponding to the C–H stretching of pyran ring of cellulose appeared around 2900 cm^{-1} . The characteristic absorption peak of cellulose I β appeared at 3270 cm^{-1} and 710 cm^{-1} . These results indicated that the sea squirt cellulose was mainly composed of I β crystal [25], also further verifying the successful preparation of sea squirt-derived cellulose hydrogels. In addition, a new peak at 1735 cm^{-1} appears in the tunic hydrogel sample, which should be corresponding to C=O stretching, which is absent for the untreated sample. The presence of C=O band indicates a portion of hydroxyl groups from cellulose in the tunic hydrogel sample was oxidized during treatment with H_2SO_4 . From the blue curve of PTC hydrogel (Fig. 2d), these typical peaks of Ppy, including C=C stretching vibration at 1546 cm^{-1} , C–N stretching vibration at 1446 cm^{-1} and the pyrrole ring at 1317 cm^{-1} , revealed that the Ppy nanoparticles were successfully bonded on the surface of cellulose fibers [26]. TGA analysis was conducted to further characterize the thermal stability and component structure of these hydrogel samples. The pristine tunic had a peak degradation temperature of 316°C and the tunic hydrogel was higher, 368°C , while the PTC hydrogel sharply increased to 394°C (Fig. 2e and f). The weight-loss ratios between 100 and 200°C were about 7.32%, 2.75% and 4.68% for pristine tunic, tunic hydrogel and PTC hydrogel, respectively. This result indicated different water content of the three groups. The decomposition of pristine tunic, tunic hydrogel and PTC hydrogel began at approximately 253°C , 294°C and 318°C , respectively. The tunic hydrogel and PTC hydrogel exhibited higher thermal stability in contrast to pristine tunic group. The pristine tunic, which contained more protein and lipid, is easier to be degraded at same high temperature, while the tunic hydrogel and PTC hydrogel processed more crystallized cellulose structures or thermally stable Ppy nanoparticles, which requires higher temperatures to destroy crystalline structure and take place degradation [9]. In the DTG curve of PTC hydrogel, the degradation temperature at 394°C was due to the thermal degradation of cellulose and Ppy polymeric chains, which was much higher than that of pristine tunic (316°C) and tunic hydrogel (368°C). This could be interpreted by the formation of uniform Ppy layer in the hydrogel caused by the electrostatic interactions and hydrogen bonding between positively charged Ppy and

cellulose fibers [27].

Porous microstructures of scaffold materials can provide a 3D microenvironment for the growth and repair of cell and tissue, which is critical for an effective cardiac patch [28]. We applied SEM to observe the morphology and porous microstructures of the tunic hydrogel and PTC hydrogels (Fig. 3, a1-a3). Compared with the compact and non-porous pristine tunic scaffold, the tunic hydrogel and PTC hydrogel exhibited a typical porous structure with a huge number of pores, which provides nutrients and oxygen for cardiomyocytes (CMs). The tunic of sea squirt was composed of protein, lipid and cellulose, which the low-porosity led to poor cell adhesion and growth [29]. After the treatment to isolate the protein, lipid and other components from the pristine tunic, porous structure was left in tunic hydrogel, ensuring sufficient 3D space for cell proliferation and growth. In addition, the fibers of tunic hydrogel possessed well-aligned and similar to the structure of myocardial tissue, which can guide CMs arrange and organization within 3D environment. Ppy nanoparticles were uniformly deposited on the surface of cellulose fibers (Fig. 3, a3), which indicates the successful modification of in-situ polymerization, also endows PTC hydrogel scaffold with a high conductivity (Fig. 3, c4).

Appropriate surface properties of scaffold materials, for example surface roughness and wettability, are also crucial for the growth and adhesion of cell [30]. AFM is applied to determine the surface roughness of the pristine tunic, tunic hydrogel and PTC hydrogel. The surface of tunic scaffold was relatively smooth, while both the tunic hydrogel and PTC hydrogel were much rough (Fig. 3, b1-b3). The root-mean-square (RMS) roughness (Rq value) of the pristine tunic, tunic hydrogel and PTC hydrogel were approximately 41.7 nm, 81 nm and 104 nm, respectively (Fig. 3, b4). The result indicated that the roughness increased after introduction of Ppy nanoparticles, which could accelerate the adhesion and growth of cells [31].

In addition, the wettability of hydrogel scaffolds is quantitatively determined via the contact angle measurement. The water contact angles of pristine tunic, tunic hydrogel and PTC hydrogel were summarized (Fig. 3, a1-a3). The pristine tunic group had a hydrophilicity surface with a contact angle of $59.32^\circ \pm 5.3^\circ$. After treatment, the contact angle of tunic hydrogel and PTC hydrogel decreased to $22^\circ \pm 3.6^\circ$ and $23^\circ \pm 1.2^\circ$ respectively, indicating that the treated scaffolds were more hydrophilic than untreated tunic scaffolds. These results showed that the tunic hydrogel and PTC hydrogel were bio-friendly to cell growth and adhesion [32].

The applicable conductivity of cardiac patch is indispensable to reconstruct the myocardial microenvironment of infarction region. Also, the e-AFM with conductive mode was applied to check the current distribution in different hydrogels. The pristine tunic showed a uniform yet low current distribution, while the tunic hydrogel processed a perfect balance with good conductivity distribution and homogenous structure (Fig. 3, c1-c3). In PTC hydrogel, a relatively strong current was distributed with the similar result of SEM (Fig. 3, a3 and c3), further indicating that conductive polymer Ppy was uniformly distributed around cellulose fiber. The homogeneity decreased while surface roughness increased with the introduction of Ppy nanoparticle, especially the current was not distributed in 0.5/PTC (0.5 mg/mL pyrrole polymerization) and 2/PTC (2 mg/mL pyrrole polymerization) hydrogel (Figs. S1a–c), throwing up barriers against a good electric stability for patch scaffolds. This may be ascribed to the too low or too high concentration of pyrrole incisively affect the in-situ reaction and distribution of the resulted Ppy nanoparticles.

Electrochemical workstation was conducted to further test the electrical conductivity of the various scaffolds. From the cyclic voltammetry (CV) curves, the area of the tunic hydrogel is larger than that of the pristine tunic and close to the area of the PTC hydrogel, indicating that the electric quantity of the tunic hydrogel is similar to that of the PTC hydrogel (Fig. S1d), which showed the same trend as the results of e-FAM. These results displayed a very interesting phenomenon that the tunic hydrogel also had relatively good conductivity of $0.076 \pm 0.016\text{ S/}$

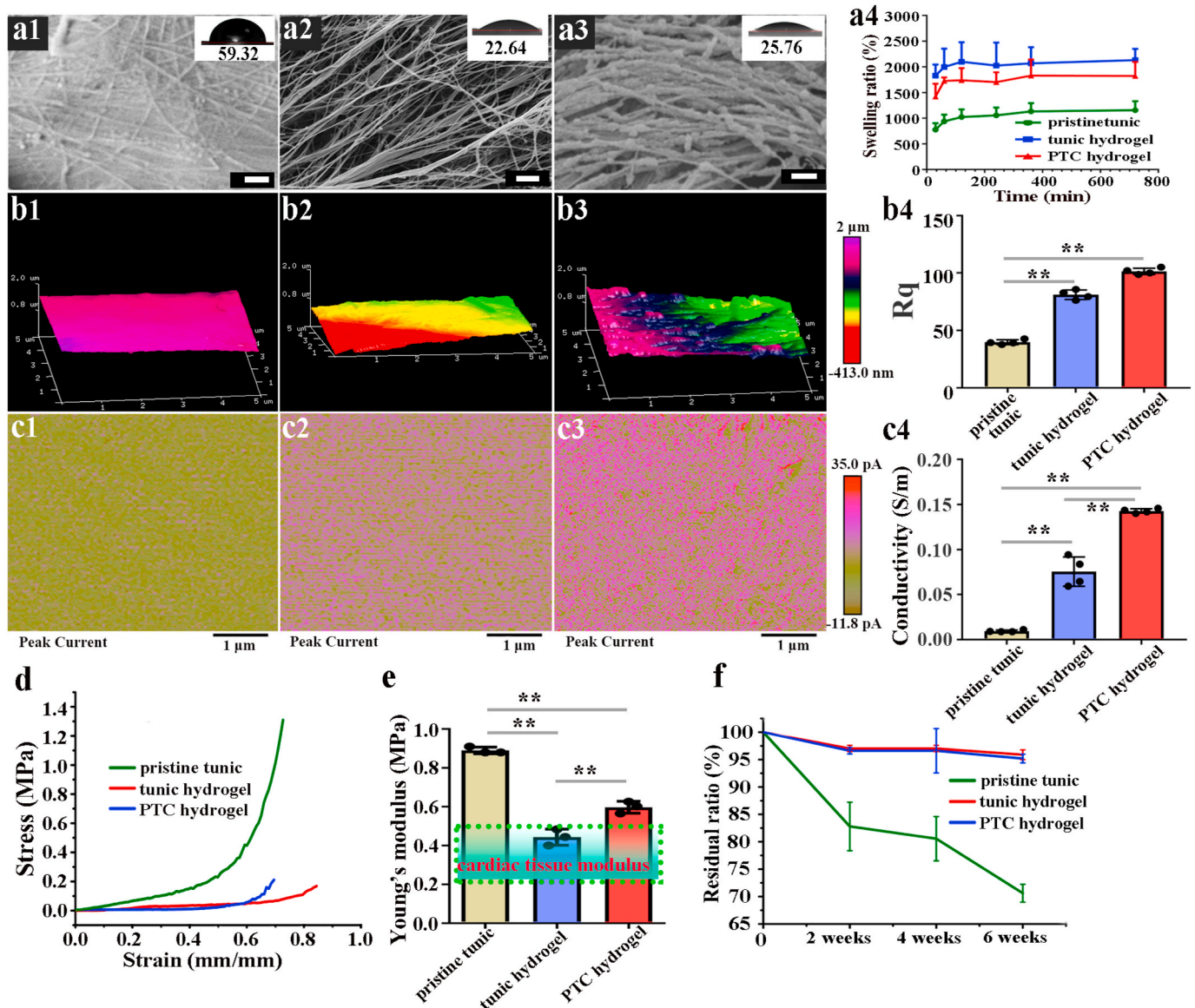


Fig. 3. The morphological, conductive and mechanical characteristics of the scaffold. The SEM images of pristine tunic (a1), tunic hydrogel (a2) and PTC hydrogel (a3), scale bars: 200 nm. The inset are corresponding photos of contact angle on the surface of samples. (a4) The uptake water analysis of pristine tunic, tunic hydrogel and PTC hydrogel $n = 4$. (b1-3) Surface morphology and (b4) corresponding surface roughness R_q of pristine tunic (b1), tunic hydrogel (b2) and PTC hydrogel (b3) revealed by AFM test. The current distribution of pristine tunic (c1), tunic hydrogel (c2) and PTC hydrogel (c3) revealed by e-AFM test, $n = 4$. (c4) Statistical analysis of conductivity in pristine tunic, tunic hydrogel and PTC hydrogel $n = 4$. (d) The stress-strain curves of pristine tunic, tunic hydrogel and PTC hydrogel. (e) The Young's modulus of pristine tunic, tunic hydrogel and PTC hydrogel $n = 3$. (f) The degradation ratio of pristine tunic, tunic hydrogel and PTC hydrogel in physiological environment $n = 4$. All data are presented as mean \pm SD. * $P < 0.05$, ** $P < 0.01$.

m in contrast to the high conductive PTC hydrogel (Fig. 3, c2-c4 and Fig. S1d). This could be explained by the following reasons. In the process of treatment with sulfuric acid and following alkali, some hydroxyl groups on the surface of fiber are oxidized to polycarboxylate ion groups, which enables the resulting tunic hydrogel with a certain of ionic conductivity. In addition, the cellulose fiber of tunic hydrogel exhibits good orientation, which further enhance electron conduction. The conductivity value of tunic hydrogel matches very well with that of native myocardial tissue (ranging from 0.005 to 0.16 S/m) [33], which meets the electrical-integration requirement of myocardial tissue and thus guarantees the potential application as a functional conductive myocardial patch.

The high specific surface area and highly porous 3D structure are important for high-density cell and tissue culture [34]. Specific surface area and pore volume of scaffolds were detected using BET and BJH

methods. The pristine tunic exhibited a specific surface area of $30.78 \text{ m}^2 \text{ g}^{-1}$, while tunic hydrogel and PTC hydrogel showed a specific surface area of 46.57 and $75.63 \text{ m}^2 \text{ g}^{-1}$, respectively (Fig. S2, d-f). A lower surface area of pristine tunic may be understood due to the densification of the protein and lipid. The Ppy nanoparticles coated the cellulose fibers of PTC hydrogel, which significantly increased the surface area. Suitable specific surface area and pore endowed the scaffold a good ability to capture water (Fig. 3, a4). The tunic hydrogel and PTC hydrogel could uptake water 18 and 20 times their initial weight, respectively, which were higher than the tunic hydrogel group. The enhanced capacity of uptake water and swelling ratio should be ascribed to the removal of proteins and lipids, which effectively formed porous structure, resulting in faster diffusion of water into the hydrogel. After a typical biological degradation experiment by being incubated in PBS for 6 weeks, the pristine tunic, tunic hydrogel and PTC hydrogel scaffolds

showed some different changes of morphological features. Some porous structure appeared on the surface of originally pore-free tunic (Fig. S2a), and the weight of the tunic decreased to 70.6% in (Fig. 3f). It could be explained that the protein and lipid of tunic degraded. Proteins and lipids degraded rapidly over time at 37 °C, and the loss of tunic mass was mainly due to the degradation of protein and lipids. When the proteins and lipids disappeared in the pristine tunic, formed holes in their original positions. The weight of tunic hydrogel and PTC hydrogel decreased slightly, while could maintain over 90% of the initial mass, thus the porous structure of them changed rarely after 6 weeks (Figs. S2, b, c and Fig. 3f), demonstrating a good structure stability. These results manifest the crystalline structure of cellulose enabled it stable for a long time, which could be used as biological scaffolds for relatively long-term stability and excellent biodegradability for tissue repair. Besides, Ppy nanoparticles remained uniformly on the surface of the cellulose fiber in PTC hydrogel without any change. In contrast, the introduction of Ppy nanoparticle provides the basis for high conductivity, but it presents hidden trouble of safety at the same time due to their non-biodegradability. Moreover, considering the requirements of biological tissue, biological scaffolds need to possess certain mechanical properties. The mechanical properties of three scaffolds were studied by using the compression test and Young's modulus method. It is showed the stress-strain curves of pristine tunic, tunic hydrogel and PTC hydrogels (Fig. 3d). Tunic hydrogel and PTC hydrogels would not crush before the compressive strain exceed 70% due to the excellent deformability. While the tunic group have poor elasticity and compressive strain is less than 50%. It is showed that the Young's modulus of pristine tunic, tunic hydrogel and PTC hydrogel was 0.89 ± 0.014 , 0.44 ± 0.034 and 0.59 ± 0.025 MPa, respectively (Fig. 3e). The Young's modulus of tunic hydrogel and PTC hydrogel were more suitable for the natural

myocardium with a modulus ranging of 0.2–0.5 MPa at the end of a diastole [35]. PTC hydrogel could be compressed freely and it recovered to its original shape immediately, showing a good elasticity and flexibility (Fig. S3b). In addition, compared with common cotton cellulose-based hydrogels from plant source (Fig. S3a), the tunic hydrogel and PTC hydrogel from animal source possessed higher Young's modulus, better elasticity and compressive capacity, which exhibited more suitability and unique advantage for cardiac patch scaffolds. These results indicated that tunic hydrogel and PTC hydrogel could be good at mimicking the native the cardiac tissue and be promising as functional patches in cardiac tissue engineering.

3.2. Cellulose hydrogel could facilitate the maturation and the functionalization of cardiomyocytes *in vitro*

In order to evaluate the biocompatibility of hydrogel, the cytotoxicity of the pristine tunic, tunic hydrogel and PTC hydrogels was assayed firstly. From the results of live/died test, the CMs grew well on three scaffolds (green), with only a few dead cells (red) (Fig. S4, a-c). In addition, all cells grew in the same direction. The result of CCK-8 showed that the cell viability of CMs exhibited no obvious difference on three different scaffolds (Fig. S4d). These results indicated that the three scaffold-derived sea squirts possessed good biocompatibility, and the inclusion of Ppy in the cellulose scaffold was not toxic. To research the cytoskeleton characteristics of the CMs, the cells on scaffolds were dyed for F-actin fibers. After being cultured 7 days, the elongated intracellular actin filaments of cytoskeleton organization of the CMs were exhibited and more cells were connected to form a network in all cellulose scaffolds (Fig. 4a). Compared to those in the pristine tunic scaffold, the CMs grew better and in greater numbers on the tunic hydrogel and PTC

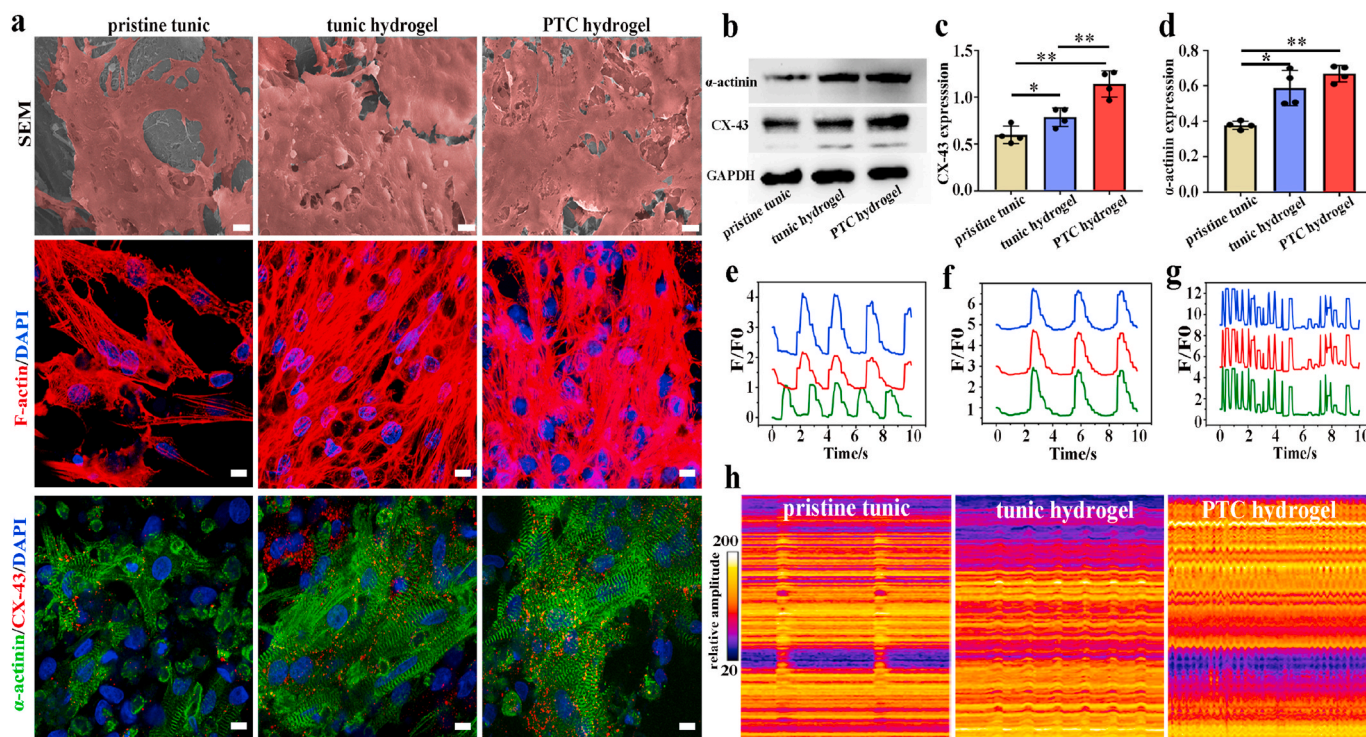


Fig. 4. The morphological and functional characteristics of cardiomyocytes in scaffolds. (a) The morphology and maturation analysis of CMs in different scaffolds at day 7 of culture. The SEM of CMs seeded on pristine tunic, tunic hydrogel and PTC hydrogel, scale bars: 50 μ m. The F-actin stained of cytoskeleton of CMs on pristine tunic, tunic hydrogel and PTC hydrogel. Expression of cardiac-specific proteins of α -actinin (green) and CX-43 (red) in the CMs on pristine tunic, tunic hydrogel and PTC hydrogel. Scale bars: 20 μ m. (b) Western blotting detection for the expressions of α -actinin protein and CX-43 protein in CMs in different scaffolds at day 7 of culture. (c–d) The quantitative proteins expression of CX-43 (c) and α -actinin (d) in CMs in different scaffolds based on western blotting detection, $n = 4$. (e–g) Calcium transient of CMs on different scaffolds at day 7 of culture. (h) The analysis of spontaneous contraction activity of CMs seeded on pristine tunic, tunic hydrogel and PTC hydrogel culture of day 7. All data are presented as mean \pm SD. * $P < 0.05$, ** $P < 0.01$. (For interpretation of the references to color in this figure legend, the reader is referred to the Web version of this article.)

hydrogel. Furthermore, the orientation of CMs was quantitatively analyzed based on fluorescence images of F-actin staining. We observed that CMs on the tunic hydrogel and PTC hydrogel showed well cell alignment parallel to the fiber direction, while the CMs on the tunic surface did not display any directionality preference (Fig. S5). The growth of the CMs and the organization of the cytoskeleton on the tunic hydrogel and PTC hydrogel are obviously directional, which is very similar to the organization of natural myocardial tissue. These results implied that the tunic cellulose derived natural scaffolds could promote the adhesion and organization of CMs.

The effects of different scaffolds for the functionalization of CMs were explored by the expression of cardiac-specific proteins, calcium transients, and synchronous contractions in different scaffolds. α -actinin, an important cardiac protein, can promote the maturation of CMs and is closely related to the synchronous contraction of the myocardium [35,36]. CX-43 is an important gap connexin which is in charge of the electrical contraction coupling of CMs and synchronous contraction of cells [37]. The CMs in three group scaffolds expressed the typical sarcomeres after being cultured for 7 days (Fig. 4a). However, compared to pristine tunic group, the sarcomeres of CMs in tunic hydrogel and PTC hydrogel showed more homogeneous alignment, highly organized intracellular. The percentages of α -actinin coverage area achieved about 50% in pristine tunic, 70% in tunic hydrogel and about 75% in PTC hydrogel after 7 day of culture, respectively (Fig. S6a). Furthermore, the expression and distribution of α -actinin and CX-43 proteins exhibited different patterns in various scaffolds: low levels around the cytomembranes in the pristine tunic, but high levels along the cytomembranes homogeneously in the tunic hydrogel and PTC hydrogel (Fig. 4, b-d). And the expression of CX-43 in PTC hydrogel was double than that of in pristine tunics (Fig. 4c). This may be explained that the higher roughness and conductivity in tunic hydrogel and PTC hydrogel can facilitate the adhesion and connection of cells. The results suggested that the tunic hydrogel and PTC hydrogel could improve the maturation and functionalization of CMs. In addition, the tunic hydrogel and PTC hydrogel could facilitate CX-43 protein of CMs and cell-cell coupling compared to the pristine tunic group, demonstrating the potential for the repair of infarcted cardiac muscles.

The most important function of CMs is spontaneous contraction. The intracellular Ca^{2+} is a key regulator of spontaneous contraction in CMs [38,39]. In order to investigate calcium activity of CMs, we tracked the calcium signal using Fluo-4 AM as the fluorescent calcium indicator [40]. The intracellular Ca^{2+} signal synchronously appeared in tunic hydrogel and PTC hydrogel after being cultured 7 days, with the simultaneous form of the parallel and rhythmic flows of Ca^{2+} at different spots (Fig. 4, e-g) (Fig. S6b, movie S1). The reason was that a functional cardiac symbiont was formed between the maturation cardiomyocytes and the three-dimensional structure in tunic hydrogel and PTC hydrogel. Specifically, Ppy endowed the cellulose fiber good conductivity, which bridged the electrically insulated structure of the matrix and facilitated electrical signal propagation between the cells. However, the intracellular Ca^{2+} spikes appeared in different frequencies at 3 individual spots in the pristine tunic. It can be explained that the number of CMs and the expression of CX-43 protein of CMs was low, which led to the weak connection of CMs. In addition, the low electrical conductivity led to the signal delay of Ca^{2+} . These results indicated that the natural self-conductive tunic hydrogel and PTC hydrogel scaffolds could promote the maturation and spontaneous contraction of CMs.

Supplementary data related to this article can be found at <https://doi.org/10.1016/j.bioactmat.2020.12.011>.

In addition, we investigate the beating behavior of CMs within scaffolds using the real-time video microscopy. All groups, on either pristine tunic scaffold or tunic hydrogel and PTC hydrogel scaffolds, demonstrated spontaneous beating activities, which mainly generated by the CMs populations in various scaffolds (Fig. 4h, Fig. S7 and movie S2). A relatively stable synchronous beating behavior were recorded in three scaffold groups. In comparison the beating frequency and

amplitude of tunic hydrogel and PTC hydrogel scaffolds were much higher than these of pristine tunic. The Ppy conductivity nanoparticles endowed the scaffold good capacity of electrical signal conduction, which could quickly conduct electrical signals generated by Ca^{2+} activity. Compared with the pristine tunic and PTC groups, the synchronous beating of tunic hydrogel was not fastest, but the beating amplitude was the most stable and rhythmical, showing the greatest potential for MI repairing. It can be explained that the elastic modulus and conductivity of the tunic hydrogels are close to these in natural cardiac tissue, which can better mimic the dynamic contractive properties of the natural myocardium than stiff scaffolds. The above results indicated that the tunic cellulose derived natural self-conductive scaffolds from sea squirts exhibited an excellent performance for facilitating the maturation of CMs, communication of cell-cell, and interaction of cell-scaffold, and enhance electrical impulse of CMs propagation across the tunic cellulose based ECP (Engineered cardiac patch) in vitro.

Supplementary data related to this article can be found at <https://doi.org/10.1016/j.bioactmat.2020.12.011>.

3.3. Tunic cellulose hydrogel derived ECPs could improve cardiac performance of rats after myocardial infarction

The aforementioned results revealed that our novel tunic cellulose derived natural self-conductive hydrogel scaffolds exhibited a promising potential for the growth of CMs and their functionalization in vitro. In order to investigate therapeutic performance of tunic cellulose hydrogel derived ECPs for the repair of MI in vivo, the myocardial infarction model was established in SD rats via ligation left anterior descending (LAD) [20]. Then, the tunic hydrogel with cardiomyocytes and PTC hydrogel with cardiomyocytes were transplanted on the infarcted myocardium for 4 weeks. The effect of these ECPs on MI rats in vivo were evaluated for the sham group (control group), the MI group, tunic hydrogel and PTC hydrogel group based on whole left ventricle structure and function using echocardiography measurements. The echocardiograph images revealed that the contractile activity and wall thickness in left anterior wall of the myocardial infarction of tunic hydrogel and PTC hydrogel group significantly enhanced (Fig. 5a). The fractional shortening (FS) and ejection fraction (EF) of MI rats significantly increased in the tunic hydrogel and PTC hydrogel compared to MI groups (Fig. 5b and c). The End Diastolic Velocity (EDV) and End Systolic Volume (ESV) were also efficiently restrain on negative left ventricle dilation in the tunic hydrogel and PTC hydrogel group, especially in tunic hydrogel group (Fig. 5d and e). Quite the contrary, the EDV and ESV in MI group is aggravated significantly, indicating a nasty and harmful infarct expansion. These results indicated that the capability of pumping blood was significantly strengthened in the tunic hydrogel and PTC hydrogel compared to MI group. The tunic cellulose hydrogel derived ECP could enhance the cardiac function and suppress harmful left ventricle remodeling after myocardial infarct.

The cardiac morphology and pathological changes in the infarct area were investigated for the control group, the MI group, tunic hydrogel and PTC hydrogel group through the Masson's Trichrome staining method [41]. As shown in Fig. 5f, the infarcted area was stuffed with fibrous tissues (blue) and the ventricular wall became very thin in MI group, while in the tunic hydrogel and PTC hydrogel possessed more myocardial tissues (red) in infarct areas compared to the MI group. The infarct size of tunic hydrogel and PTC hydrogel significantly decreased compared to MI group, the infarct size was $53.59\% \pm 2.28\%$ in MI group, $21.78\% \pm 3.81\%$ in tunic hydrogel group and $22.96\% \pm 2.46\%$ in PTC hydrogel group. Compared with the MI group, the thickness of ventricle walls increased in tunic hydrogel and PTC hydrogel group, which could possess stronger contraction capacity.

The electric-contraction coupling in the infarcted area after the different patches transplantation were assessed through detecting the α -actinin and CX-43 protein levels using immunofluorescence staining [42]. Compared to the MI groups, a more organized-actinin positive

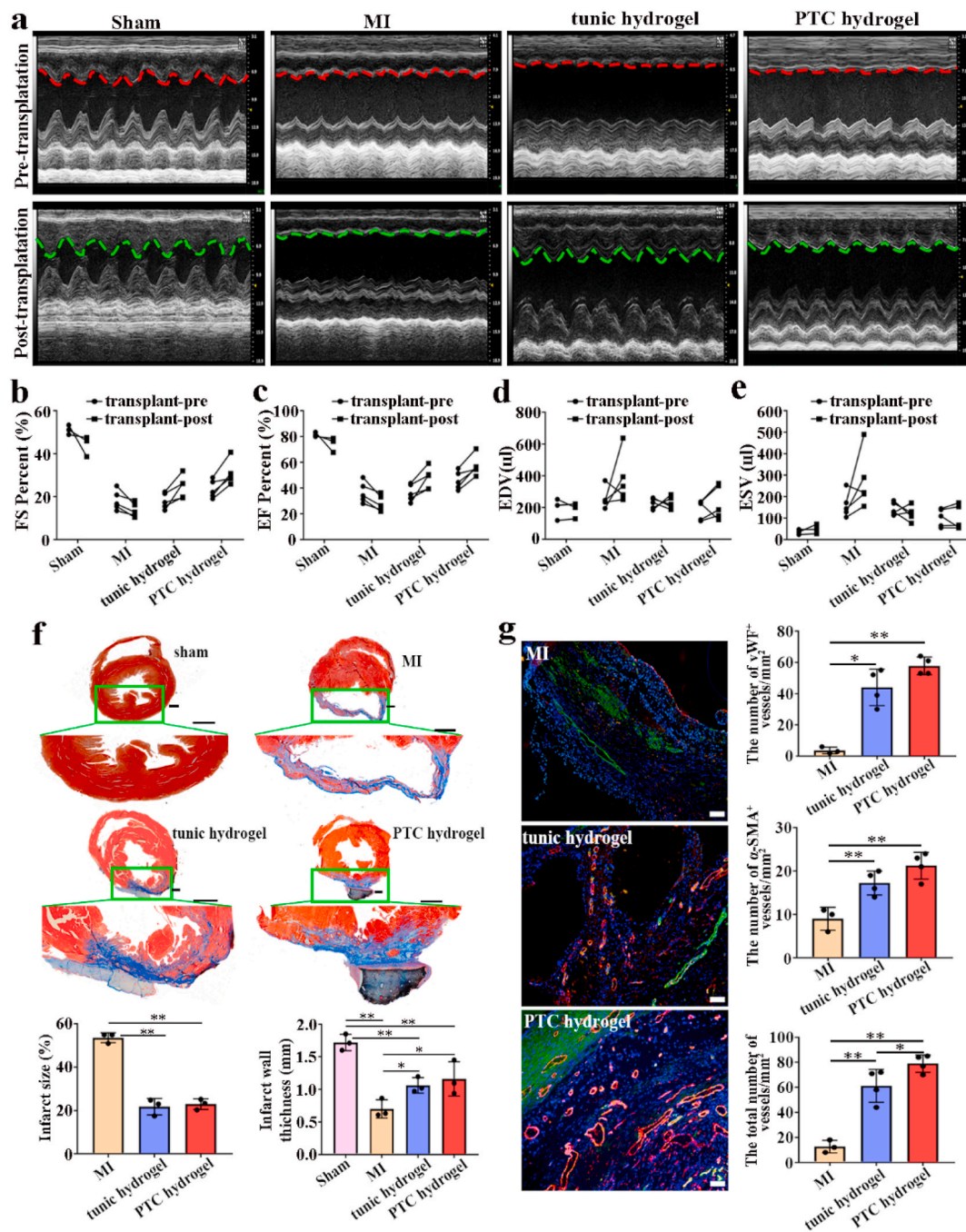


Fig. 5. Repair effect of patch in myocardial infarction rats. (a) The echocardiographic images of pretransplant (above) and posttransplant (bottom) in the sham group (control group), the MI group, tunic hydrogel and PTC hydrogel group. (b–e) Representative parameters of left ventricular function based on echocardiography of different groups after 4 weeks of implantation. (f) Masson's staining displayed the fibrous tissue (blue) and myocardium (red) of sections of hearts from animals in different groups. Scale bars: 1 mm. Statistical analysis of infarct size and infarct wall thickness of the infarcted heart in different group (bottom), $n = 3$. (g) vWF immunostaining (red) and α -SMA immunostaining (green) within infarcted area in different groups, $n = 4$. Scale bars: 50 μ m. The different microvessel densities within infarcted region in different groups based on vWF/ α -SMA immunostaining staining. All data are presented as mean \pm SD. * $P < 0.05$, ** $P < 0.01$. (For interpretation of the references to color in this figure legend, the reader is referred to the Web version of this article.)

myocardium and enhanced expression of CX-43 were detected in the infarcted area of the tunic hydrogel and PTC hydrogel implanted rats (Fig. S8). The healthy and MI regions were bridged using a favorable ECP, which could support the structural integrity and regeneration of tissues in MI. The scaffolds with conductive polymer composite can improve the cardiac function of the infarcted heart by accelerating the conduction velocity and repolarization around the infarcted area, and help to restore the lost electrical conductivity and synchronous contraction of scar tissue [43]. But in this work, it is very interesting

that, the tunic hydrogel without conductivity polymer also could enhance the cardiac function. These results showed that the hydrogel from sea squirts cellulose could promote the repair of myocardial infarction and a desirable repair efficacy for MI rats.

The participation of inflammatory microenvironment in the MI repair is another big concern. Previous studies have shown that M1 macrophages secrete pro-inflammatory cytokines to accelerate the formation of myocardial infarction fibrosis, while M2 macrophages inhibit the release of pro-inflammatory cytokines and contribute to the repair of

the disease [44]. Herein, we investigated whether the inflammatory microenvironment participate in the repair effect of tunic cellulose hydrogel derived from sea squirts for the control group, the MI group, tunic hydrogel and PTC hydrogel group. In the infarction region of the MI rats, CD68 positive pro-inflammatory macrophages would cause a detrimental inflammatory response and expedite the fibrosis. Our results showed that expression of CD68 were lower in tunic hydrogel and PTC hydrogel groups than the MI group indicated that few M1 macrophages located in the infarct region in the patches transplantation group (Fig. S9). Meanwhile, the expression of pro-healing M2 macrophages specific marker MRC1 were significantly higher in the two hydrogels group than the MI group. The results revealed that the inflammatory possible participate the infarction repair of tunic hydrogel and PTC hydrogel.

The angiogenesis is crucial in MI repair and regeneration. The newborn vascular system could restore blood flow, which provides nutrients and oxygen for the infarcted area [45]. The promotion angiogenesis could delay the occurrence of ventricular remodeling after myocardial infarction. It is necessary that the functional ECP could facilitate the vascularization in the infarct area. In order to evaluate the vascularization in infarct region, the vWF for endothelial and α -SMA for vascular smooth muscle cell were tested through immunofluorescence staining. Compared to the MI, the tunic hydrogel and PTC hydrogel groups showed that the number of functional vascular was significantly increase (Fig. 5g). Abundant capillaries (vWF⁺) and arteriole (vWF⁺/ α -SMA⁺) in the tunic hydrogel-derived ECP and PTC hydrogel-derived ECP could provide adequate nutrients and oxygen for cells in infarcted area, which could avoid the cell dead. In addition, this neovascularization system could expel harmful products from the infarct area, preventing more cell death and the enlargement of the infarct area [46]. In this study, the tunic hydrogel and PTC hydrogel scaffolds could promote angiogenesis and provide suitable microenvironment, which could delay the progression of infarction.

4. Conclusions

In conclusion, we presented a novel strategy to settle a more and more serious biofouling issue induced by the overpopulation of symbiont tunicates in marine culturing industry. We firstly demonstrated the ability to upgrade the tunic from marine aquaculture waste-sea squirt and explored a new way of successful application of sea squirt tunic-derived hydrogel as a functional patch scaffold in cardiac tissue engineering. The porous, flexible and self-conductive cellulose hydrogel with well-aligned nanofibers were directly obtained from the tunic of sea squirts through a modified bio-refining method, which can remove the immunogenic constituent protein and lipid while retain the intrinsic structure and physicochemical and biologic properties of tunic and enabling it advantageous for broad fields, especially in bio-applications. Distinguishing from these published works using the pure cellulose or their nanocrystals from the tunic, we focused on the holistic material of tunic hydrogel. As far as we know, this is the first example of a bio-refining natural self-conductive sea squirt tunic-derived hydrogel with excellent biocompatibility, suitable conductivity/mechanical properties and well-aligned fiber structure similar with that of native cardiac tissue. This ability is in stark contrast to that of conventional synthetic or conductive-additive doped natural systems seen in the literature, in which the biocompatibility, biodegradability and tissue-rejection are rather limited and poorly controlled. This elegant and simple development of this method allows performing well-aligned fiber structure similar with that of native cardiac tissue, excellent biocompatibility and suitable conductivity of the resulted animal-derived tunic hydrogel, thus resulting in it being able to be directly applied as natural conductive patches without any conductive additives. We combined *in vitro* and animal experimental approaches to demonstrate perfect performance for significantly enhancing the cardiac function of MI rats and facilitating the repair and angiogenesis of infarcted cardiac tissues. Also, the

natural conductive products by simple refining guarantees the electrical stability and integration capability for the repair and regeneration of infarcted cardiac tissue. It can be predicted that the successful application for scaffold materials using the ocean culturing waste can substantially decrease the excessive growth induced bio-pollution and economic issue considering the large-scale consumption requirement for not only cardiac tissue engineering, but also skeletal muscle, skin, nerve and bone tissue engineering. The concepts of sustainable development we exploit here are eco-friendly, fundamental and versatile, and we expect there to be extensive future work based on this work in generalizing the work to other culturing concomitants, and in using our strategy to address the biofouling issues induced by overpopulation or other incentives. We also believe our work has significant relevance to applied fields such as biomass refining for biomedicine, catalyst carrier, cosmetics, and so on.

Author contributions

X. Z. Qiu conceived the project; X. Z. Qiu, Y. T. He, H. H. Hou and S. Q. Wang designed the experiments; Y. T. He, S. Q. Wang and R. R. Lin performed both *in vitro* and *in vivo* experiments; Y. T. He and H. H. Hou analyzed the data; X. Z. Qiu, Y. T. He and H. H. Hou interpreted the data and wrote the manuscript. L. Y. Wang and L. Yu oversaw the experiments; X. Z. Qiu and H. H. Hou oversaw all phases of the project and obtained research funding. Y. T. He, H. H. Hou and S. Q. Wang contributed equally to this work.

Declaration of competing interest

The authors have declared that no competing interest exists.

Acknowledgments

We thank the staff from the Guangdong Provincial Key Laboratory of Construction and Detection in Tissue Engineering, Department of Anatomy, School of Basic Medical Sciences, Southern Medical University, and Guangdong Province Key Laboratory of Marine Biotechnology, Shantou University. Funding: This work was supported by the National Natural Science Foundation of China (32071363, 52003113, U1601221), Science and Technology Projects of Guangzhou City (201804020035) and Guangdong Province Science and Technology Projects (2016B090913004). Key Research & Development Program of Guangzhou Regenerative Medicine and Health Guangdong Laboratory (2018GZR110104002).

Appendix A. Supplementary data

Supplementary data to this article can be found online at <https://doi.org/10.1016/j.bioactmat.2020.12.011>.

References

- [1] H. Hoag, Invaders leave enemies behind, *Nature* 6 (2003) 1476–4687, <https://doi.org/10.1038/news030203-6>.
- [2] E. Lacoste, N. Gaertner-Mazouni, Biofouling impact on production and ecosystem functioning: a review for bivalve aquaculture, *Rev. Aquacult.* 7 (2015) 187–196, <https://doi.org/10.1111/raq.12063>.
- [3] J.M. Kenworthy, D. Davoult, C. Lejeune, Compared stress tolerance to short-term exposure in native and invasive tunicates from the NE Atlantic: when the invader performs better, *Marine Biology* 165 (2018) 164, <https://doi.org/10.1007/s00227-018-3420-1>.
- [4] M.S. Islam, M. Haque, The mangrove-based coastal and nearshore fisheries of Bangladesh: ecology, exploitation and management, *Rev. Fish Biol. Fish.* 14 (2004) 153–180, <https://doi.org/10.1007/s11160-004-3769-8>.
- [5] M.J. Dunlop, A. Bishnu, B. Rabin, Isolation of nanocrystalline cellulose from tunicates, *J Environ Chem Eng* 6 (2018) 4408–4412, <https://doi.org/10.1016/j.jece.2018.06.056>.
- [6] E. Ternon, L. Zarate, S. Chenesseau, J. Croué, R. Dumollard, M.T. Suzuki, O. P. Thomas, Spherulization as a process for the exudation of chemical cues by the

- encrusting sponge *C. crambe*, *Sci. Rep.* 6 (2016) 29474, <https://doi.org/10.1038/srep29474>.
- [7] F.M. Kerton, Y. Liu, K.W. Omari, K. Hawboldt, Green chemistry and the ocean-based bio-refinery, *Green Chem.* 15 (2013) 860–871, <https://doi.org/10.1039/C3GC36994C>.
- [8] R. Cao, W. Peng, Z. Wang, A. Xu, β -Carboline alkaloids: biochemical and pharmacological functions, *Curr. Med. Chem.* 14 (2007) 479–500, <https://doi.org/10.2174/092986707779940998>.
- [9] Y. Zhao, C. Moser, G. Henriksson, Transparent composites made from tunicate cellulose membranes and environmentally friendly polyester, *ChemSusChem* 11 (2018) 1728–1735, <https://doi.org/10.1002/cssc.201800627>.
- [10] R. Ajdari, S. Huan, N. Zanjanzadeh Ezazi, W. Xiang, R. Grande, H.A. Santos, O. J. Rojas, Acetylated nanocellulose for single-component bioinks and cell proliferation on 3D-printed scaffolds, *Biomacromolecules* 20 (2019) 2770–2778, <https://doi.org/10.1021/acs.biomac.9b00527>.
- [11] H. Luo, R. Cha, J. Li, W. Hao, Y. Zhang, F. Zhou, Advances in tissue engineering of nanocellulose-based scaffolds: a review, *Carbohydr. Polym.* 224 (2019) 115144, <https://doi.org/10.1016/j.carbpol.2019.115144>.
- [12] F. Robbati, I. Sterner, S. Bottan, J.M. Monné Rodríguez, G. Pellegrini, T. Schmidt, V. Falk, D. Poulidakos, A. Ferrari, C. Starck, Microengineered biosynthesized cellulose as anti-fibrotic in vivo protection for cardiac implantable electronic devices, *Biomaterials* 229 (2020), 119583, <https://doi.org/10.1016/j.biomaterials.2019.119583>.
- [13] M.A. Laflamme, C.E. Murry, Heart regeneration, *Nature* 473 (2011) 326–335, <https://doi.org/10.1038/nature10147>.
- [14] X. Lin, Y. Liu, A. Bai, H. Cai, Y. Bai, W. Jiang, H. Yang, X. Wang, L. Yang, N. Sun, H. Gao, A viscoelastic adhesive epicardial patch for treating myocardial infarction, *Nat Biomed Eng* 3 (2019) 632–643, <https://doi.org/10.1038/s41551-019-0380-9>.
- [15] B.W. Walker, R.P. Lara, C.H. Yu, E.S. Sani, W. Kimball, S. Joyce, N. Annabi, Engineering a naturally-derived adhesive and conductive cardiopatch, *Biomaterials* 207 (2019) 89–101, <https://doi.org/10.1016/j.biomaterials.2019.03.015>.
- [16] M. Yanamandala, W. Zhu, D.J. Garry, T.J. Kamp, J.M. Hare, H.W. Jun, Y.S. Yoon, N. Bursac, S.D. Prabhu, G.W. Dorn, R. Bolli, R.N. Kitsis, J. Zhang, Overcoming the roadblocks to cardiac cell therapy using tissue engineering, *J. Am. Coll. Cardiol.* 70 (2017) 766–775, <https://doi.org/10.1016/j.jacc.2017.06.012>.
- [17] J.B. Hu, M.L. Tomov, J.W. Buikema, C. Chen, M. Mahmoudi, S.M. Wu, Cardiovascular tissue bioprinting: physical and chemical processes, *Appl. Phys. Rev.* 5 (2018), 041106, <https://doi.org/10.1063/1.5048807>.
- [18] Y. Wu, L. Wang, B. Guo, P.X. Ma, Interwoven aligned conductive nanofiber yarn/hydrogel composite scaffolds for engineered 3D cardiac anisotropy, *ACS Nano* 11 (2017) 5646–5659, <https://doi.org/10.1021/acsnano.7b01062>.
- [19] M.T.I. Mredha, H.H. Le, V.T. Tran, P. Trtik, J.X. Cui, I. Jeon, Anisotropic tough multilayer hydrogels with programmable orientation, *Mater Horiz* 6 (2019) 1504–1511, <https://doi.org/10.1039/C9MH00320G>.
- [20] L.Y. Wang, J.Z. Jiang, W.X. Hua, A. Darabi, X.P. Song, C. Song, W. Zhong, M.Q. M. Xing, X.Z. Qiu, Mussel-inspired conductive cryogel as cardiac tissue patch to repair myocardial infarction by migration of conductive nanoparticles, *Adv. Funct. Mater.* 26 (2016) 4293–4305, <https://doi.org/10.1002/adfm.201505372>.
- [21] M.M. Pakulska, K. Vulic, R.Y. Tam, M.S. Shoichet, Hybrid crosslinked methylcellulose hydrogel: a predictable and tunable platform for local drug delivery, *Adv Mater* 27 (2015) 5002–5008, <https://doi.org/10.1002/adma.201502767>.
- [22] J.A. Infant, feeding, The physiological basis, *Bull. World Health Organ.* (1989) 1–108.
- [23] C.M. Weaver, Calcium requirements of physically active people, *Am. J. Clin. Nutr.* 72 (2000) 579–584, <https://doi.org/10.1093/ajcn/72.2.579S>.
- [24] Ha-W An, Highly conductive and stretchable conductors fabricated from bacterial cellulose, *NPG Asia Mater.* 4 (2012) e19, <https://doi.org/10.1038/am.2012.34>.
- [25] L.M. Cao, X.F. Fu, C.H. Xu, S.H. Yin, Y.K. Chen, High-performance natural rubber nanocomposites with marine biomass (tunicate cellulose), *Cellulose* 24 (2017) 2849–2860, <https://doi.org/10.1007/s10570-017-1293-y>.
- [26] F. Lin, R. Zheng, J. Chen, W. Su, B. Dong, C. Lin, B. Huang, B. Lu, Microfibrillated cellulose enhancement to mechanical and conductive properties of biocompatible hydrogels, *Carbohydr. Polym.* 205 (2019) 244–254, <https://doi.org/10.1016/j.carbpol.2018.10.037>.
- [27] K. Jradi, B. Bideau, B. Chabot, C. Daneault, Characterization of conductive composite films based on TEMPO-oxidized cellulose nanofibers and polypyrrole, *J. Mater. Sci.* 47 (2012) 3752–3762, <https://doi.org/10.1007/s10853-011-6226-9>.
- [28] G.C. Engelmayr, M. Cheng, C.J. Bettinger, J.T. Borenstein, R. Langer, L.E. Freed, Accordion-like honeycombs for tissue engineering of cardiac anisotropy, *Nat. Mater.* 7 (2008) 1003–1010, <https://doi.org/10.1038/nmat2316>.
- [29] S. Bagherifard, D.J. Hickey, A.C. de Luca, V.N. Malheiro, A.E. Markaki, M. Guagliano, T.J. Webster, The influence of nanostructured features on bacterial adhesion and bone cell functions on severely shot peened 316L stainless steel, *Biomaterials* 73 (2015) 185–197, <https://doi.org/10.1016/j.biomaterials.2015.09.019>.
- [30] L. Bacakova, E. Filova, M. Parizek, T. Ruml, V. Svorcik, Modulation of cell adhesion, proliferation and differentiation on materials designed for body implants, *Biotechnol. Adv.* 29 (2011) 739–767, <https://doi.org/10.1016/j.biotechadv.2011.06.004>.
- [31] S.S. Dhadwar, T. Bemman, W.A. Anderson, P. Chen, Yeast cell adhesion on oligopeptide modified surfaces, *Biotechnol. Adv.* 21 (2003) 395–406, [https://doi.org/10.1016/S0734-9750\(03\)00056-9](https://doi.org/10.1016/S0734-9750(03)00056-9).
- [32] H. Cha, J. Ma, Y.S. Kim, L. Li, L. Sun, J. Tong, N. Miljkovic, In situ droplet microgoniometry using optical microscopy, *ACS Nano* 13 (2019) 13343–13353, <https://doi.org/10.1021/acsnano.9b06687>.
- [33] T.H. Qazi, R. Rai, D. Dippold, J.E. Roether, D.W. Schubert, E. Rosellini, N. Barbani, A.R. Boccacini, Development and characterization of novel electrically conductive PANI-PGS composites for cardiac tissue engineering applications, *Acta Biomater.* 10 (2014) 2434–2445, <https://doi.org/10.1016/j.actbio.2014.02.023>.
- [34] M. Verdanova, B. Rezek, A. Broz, E. Ukrainsev, O. Babchenko, A. Artemenko, T. Izak, A. Kromka M. Kalbac, M. Hubalek Kalbacova, Nanocarbon allotropes-graphene and nanocrystalline diamond-promote cell proliferation, *Small* 12 (2016) 2499–2509, <https://doi.org/10.1002/sml.201503749>.
- [35] X.P. Song, J. Mei, G.L. Ye, L.Y. Wang, A. Ananth, L. Yu, X.Z. Qiu, In situ pPy-modification of chitosan porous membrane from mussel shell as a cardiac patch to repair myocardial infarction, *Appl. Mater. Today* 15 (2019) 87, <https://www.sciencedirect.com/science/article/pii/S2352940718307558>.
- [36] M. Kapnisi, C. Mansfield, C. Marijon, A.G. Guex, F. Perbellini, I. Bardi, E. J. Humphrey, J.L. Puetzer, D. Mawad, D.C. Koutsogeorgis, D.J. Stuckey, C. M. Terracciano, S.E. Harding, M.M. Stevens, Auxetic cardiac patches with tunable mechanical and conductive properties toward treating myocardial infarction, *Adv. Funct. Mater.* 28 (2018), 1800618, <https://doi.org/10.1002/adfm.201800618>.
- [37] B.W. Walker, R.P. Lara, C.H. Yu, E.S. Sani, W. Kimball, S. Joyce, N. Annabi, Engineering a naturally-derived adhesive and conductive cardiopatch, *Biomaterials* 207 (2019) 89–101, <https://doi.org/10.1016/j.biomaterials.2019.03.015>.
- [38] J. Han, B. Kim, J.Y. Shin, S. Ryu, M. Noh, J. Woo, J.S. Park, Y. Lee, N. Lee, T. Hyeon, D. Choi, B.S. Kim, Iron oxide nanoparticle-mediated development of cellular gap junction crosstalk to improve mesenchymal stem cells' therapeutic efficacy for myocardial infarction, *ACS Nano* 9 (2015) 2805–2819, <https://doi.org/10.1021/nn506732n>.
- [39] S. Luongo Timothy, P. Lambert Jonathan, Gross Polina, Nwokedi Mary, A. Lombardi Alyssa, Shanmughapriya Santhanam, C. Carpenter April, Kolmetzky Devin, Gao Erhe, Van Berlo, H. Jop, The mitochondrial Na/Ca exchanger is essential for Ca homeostasis and viability, *Nature* 545 (2017) 93–97, <https://doi.org/10.1038/nature22082>.
- [40] D. Son, S.Y. Park, B. Kim, J.T. Koh, T.H. Kim, S. An, D. Jang, G.T. Kim, W. Jhe, S. Hong, Nanoneedle transistor-based sensors for the selective detection of intracellular calcium ions, *ACS Nano* 5 (2011) 3888–3895, <https://pubs.acs.org/doi/abs/10.1021/nn200262u>.
- [41] S. Liang, Y. Zhang, H. Wang, Z. Xu, J. Chen, R. Bao, B. Tan, Y. Cui, G. Fan, W. Wang, W. Wang, W. Liu, Paintable and rapidly bondable conductive hydrogels as therapeutic cardiac patches, *Adv Mater* 30 (2018), e1704235, <https://doi.org/10.1002/adma.201704235>.
- [42] W. Roell, T. Lewalter, P. Sasse, Y.N. Tallini, B.R. Choi, M. Breitbach, R. Doran, U. M. Becher, S.M.H. wang, T. Bostani, J. von Maltzahn, A. Hofmann, S. Reining, B. Eiberger, B. Gabris, A. Pfeifer, A. Welz, K. Willecke, G. Salama, J.W. Schrickel, M.I. Kotlikoff, B.K. Fleischmann, Engraftment of connexin 43-expressing cells prevents post-infarct arrhythmia, *Nature* 450 (2007) 819–824, <https://doi.org/10.1038/nature06321>.
- [43] A. Mihic, Z. Cui, J. Wu, G. Vlacic, Y. Miyagi, S.H. Li, S. Lu, H.W. Sung, R.D. Weisel, R.K. Li, A Conductive polymer hydrogel supports cell electrical signaling and improves cardiac function after implantation into myocardial infarct, *Circulation* 132 (2015) 772–784, <https://doi.org/10.1161/CIRCULATIONAHA.114.014937>.
- [44] Y. Ma, R.P. Iyer, K.Y. DeLeon-Pennell, A. Yabluchanskiy, M.R. Garrett, M. L. Lindsey, IL-10 improves cardiac remodeling after myocardial infarction by stimulating M2 macrophage polarization and fibroblast activation, *Basic Res. Cardiol.* 112 (3) (2017), <https://doi.org/10.1007/s00395-017-0622-5>.
- [45] S.K. Vemuri, S.K. Nethi, R.R. Banala, P.V.S. Goli, V.G.R. Annareddy, C.R. Patra, Europium hydroxide nanorods (EHNs) ameliorate isoproterenol-induced myocardial infarction: an in vitro and in vivo investigation, *ACS Appl. Mater. Interfaces* 2 (2019) 1078–1087, <https://doi.org/10.1021/acsabm.8b00669>.
- [46] C.V. Bouten, P.Y. Dankers, A. Triessen-Mol, S. Pedron, A.M. Brizard, F.P. Baaijens, Substrates for cardiovascular tissue engineering, *Adv. Drug Deliv. Rev.* 63 (2011) 221–241, <https://doi.org/10.1016/j.addr.2011.01.007>.